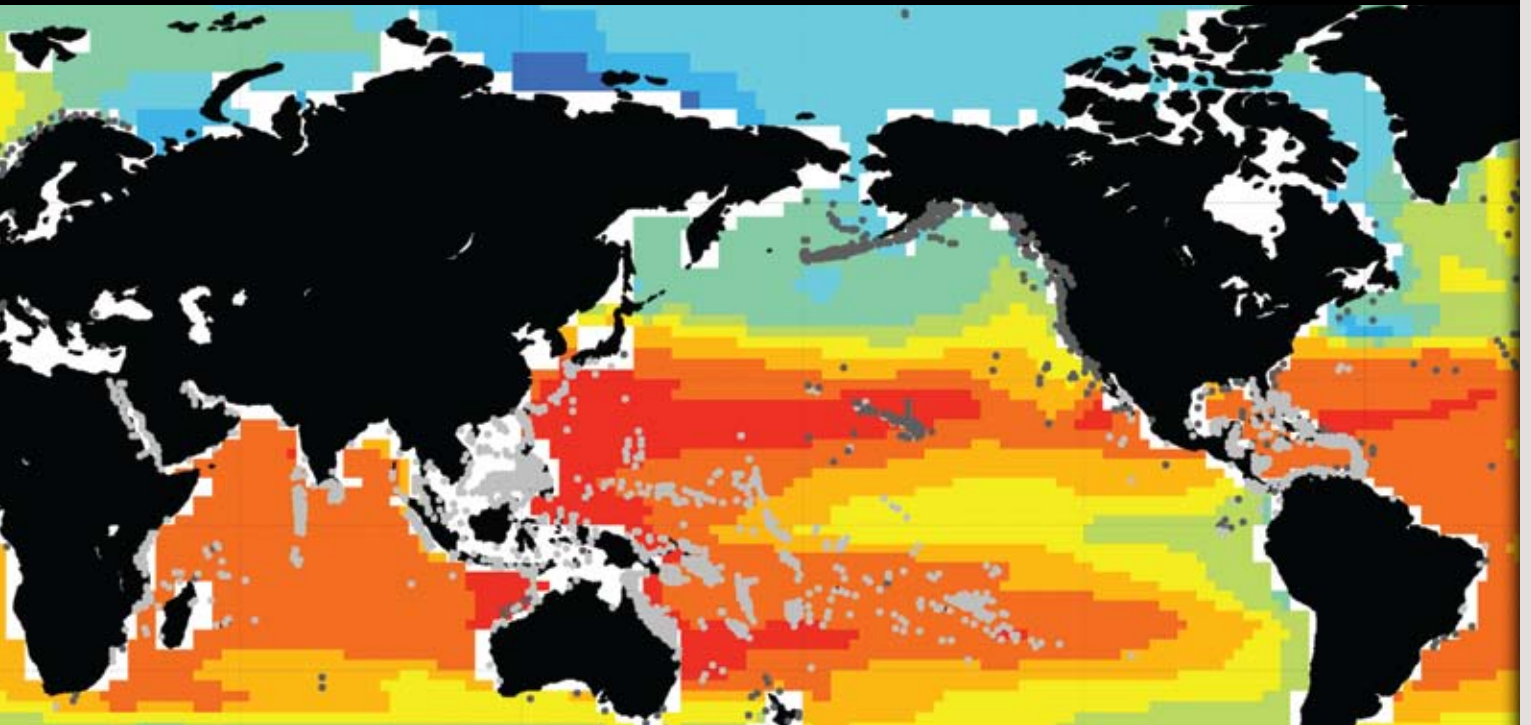BY RICHARD A. FEELY, SCOTT C. DONEY, AND SARAH R. COOLEY

Ocean Acidification

Present Conditions and Future Changes in a High-CO$_2$ World

ABSTRACT

The uptake of anthropogenic CO_2 by the global ocean induces fundamental changes in seawater chemistry that could have dramatic impacts on biological ecosystems in the upper ocean. Estimates based on the Intergovernmental Panel on Climate Change (IPCC) business-as-usual emission scenarios suggest that atmospheric CO_2 levels could approach 800 ppm near the end of the century. Corresponding biogeochemical models for the ocean indicate that surface water pH will drop from a pre-industrial value of about 8.2 to about 7.8 in the IPCC A2 scenario by the end of this century, increasing the ocean's acidity by about 150% relative to the beginning of the industrial era. In contemporary ocean water, elevated CO_2 will also cause substantial reductions in surface water carbonate ion concentrations, in terms of either absolute changes or fractional changes relative to pre-industrial levels. For most open-ocean surface waters, aragonite undersaturation occurs when carbonate ion concentrations drop below approximately 66 $\mu mol\ kg^{-1}$. The model projections indicate that aragonite undersaturation will start to occur by about 2020 in the Arctic Ocean and 2050 in the Southern Ocean. By 2050, all of the Arctic will be undersaturated with respect to aragonite, and by 2095, all of the Southern Ocean and parts of the North Pacific will be undersaturated. For calcite, undersaturation occurs when carbonate ion concentration drops below 42 $\mu mol\ kg^{-1}$. By 2095, most of the Arctic and some parts of the Bering and Chukchi seas will be undersaturated with respect to calcite. However, in most of the other ocean basins, the surface waters will still be saturated with respect to calcite, but at a level greatly reduced from the present.

INTRODUCTION

Since the beginning of the industrial revolution in the mid-eighteenth century, the release of carbon dioxide (CO_2) from humankind's combined industrial and agricultural activities has resulted in an increase in atmospheric CO_2 concentrations from approximately 280 to 387 parts per million (ppm), with as much as 50% of the increase occurring in the last three decades. Earth's atmospheric concentration of CO_2 is now higher than it has been for more than 800,000 years (Lüthi et al., 2008), and it is expected to continue to rise at an accelerating rate, leading to significant temperature increases in the atmosphere and the surface ocean in the coming decades. Over the industrial era, the ocean has absorbed about one-quarter of anthropogenic carbon emissions (Sabine and Feely, 2007; Canadell et al., 2007). This absorption has benefited humankind by significantly curtailing the growth of CO_2 levels in the atmosphere, thereby reducing the global warming realized to date.

However, when the anthropogenic CO_2 is absorbed by seawater, chemical reactions occur that reduce seawater pH, carbonate ion (CO_3^{2-}) concentration, and saturation states of the biologically important $CaCO_3$ minerals calcite (Ω_{ca}) and aragonite (Ω_{ar}) in a process commonly referred to as "ocean acidification" (Broecker and Clarke, 2001; Caldeira and Wickett, 2003, 2005; Orr et al., 2005; Doney et al., 2009; Figure 1). The pH of ocean surface waters has already decreased by about 0.1 since the industrial era began (Caldeira and Wickett, 2003,

2005; Orr et al., 2005), with a decrease of ~ 0.0018 yr^{-1} observed over the last quarter century at several open-ocean time-series sites (Bates, 2007; Bates and Peters, 2007; Santana-Casiano et al., 2007; Dore et al., 2009). By the middle of this century, atmospheric CO_2 levels could reach more than 500 ppm, and exceed 800 ppm by the end of the century (Friedlingstein et al., 2006). These CO_2 levels would result in an additional decrease in surface water pH of 0.3 units from current conditions, 0.4 from pre-industrial, by 2100, which represents an increase in the ocean's hydrogen ion (H^+) concentration by 2.5 times relative to the beginning of the industrial era. Results from large-scale ocean CO_2 surveys and time-series studies over the past two decades show that ocean acidification is a predictable consequence of rising atmospheric CO_2 (Feely et al., 2004; Bates and Peters, 2007; Santana-Casiano et al., 2007; Dore et al., 2009; Takahashi et al., 2009) that is independent of the uncertainties and outcomes of climate change.

Seawater carbonate chemistry is governed by a series of abiotic chemical reactions (CO_2 dissolution, acid/base chemistry) and biologically mediated reactions (photosynthesis, respiration, and $CaCO_3$ precipitation and dissolution). The first key reaction occurs when CO_2 gas from the atmosphere dissolves into seawater:

$$CO_2(atm) \rightleftarrows CO_2(aq). \qquad (1)$$

This exchange is relatively rapid, with atmosphere-ocean equilibration on a time scale of several months, so that surface waters in most ocean regions increase in CO_2 concentration from year to year in proportion to the increased
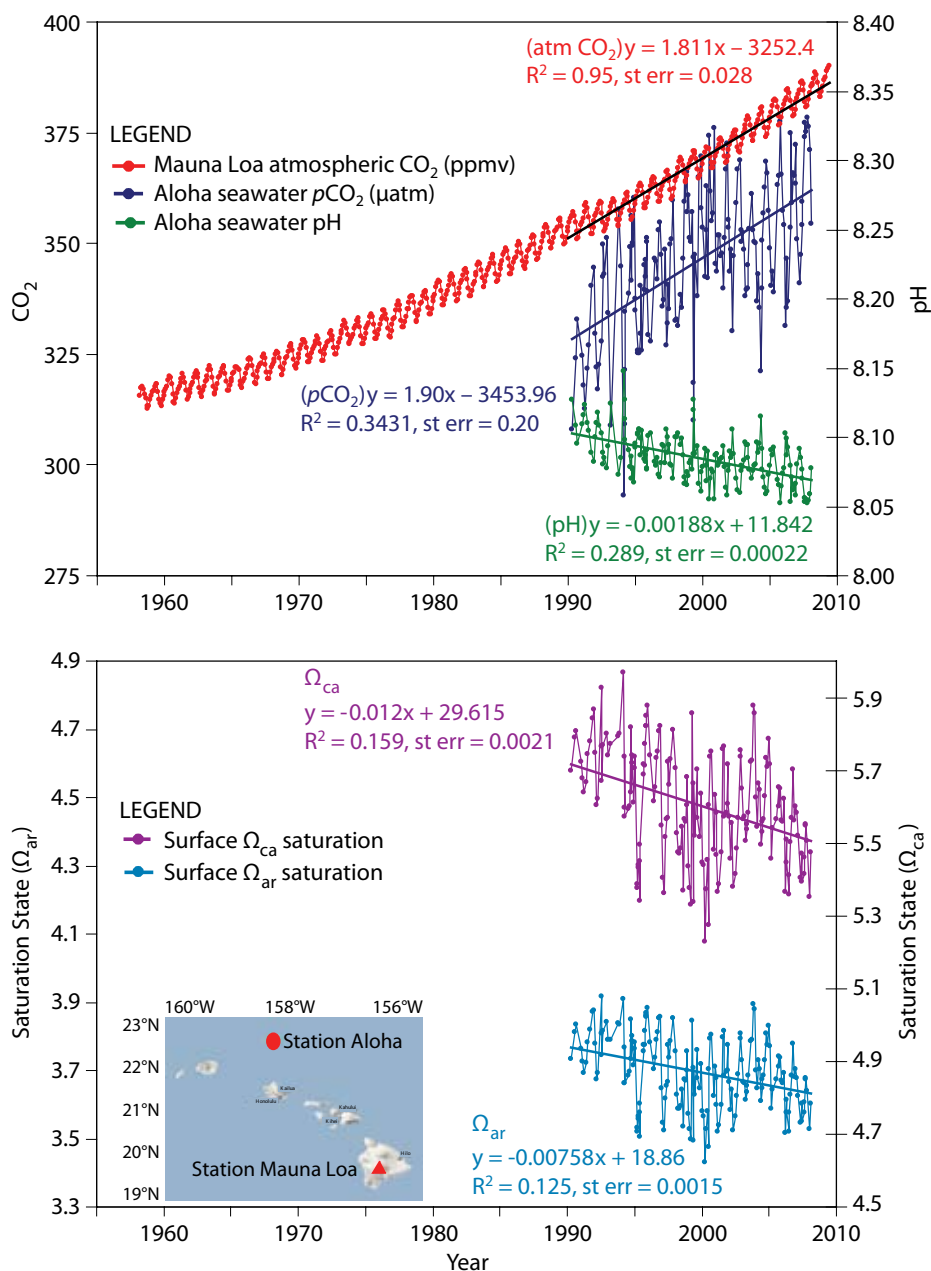
Figure 1. (Top) Time series of atmospheric CO_2 at Mauna Loa (ppmv) and surface ocean pH and pCO_2 (µatm) at Ocean Station Aloha in the subtropical North Pacific Ocean (see inset map). Note that the increase in oceanic CO_2 over the period of observations is consistent with the atmospheric increase within the statistical limits of the measurements. (Bottom) Calcite and aragonite saturation data for surface waters. *Mauna Loa data: Pieter Tans, NOAA/ESRL, http://www.esrl.noaa.gov/gmd/ccgg/trends. HOT/ALOHA data: David Karl, University of Hawaii, http://hahana.soest.hawaii.edu. Updated from Doney et al. (2009). See also Dore et al. (2009).*

CO_2 concentration in the atmosphere. The second set of reactions involves the hydration of water to form H_2CO_3, which dissociates in subsequent acid-base reactions:

$$CO_2(aq) + H_2O \rightleftarrows H_2CO_3 \rightleftarrows H^+ + HCO_3^- \rightleftarrows 2H^+ + CO_3^{2-}. \quad (2)$$
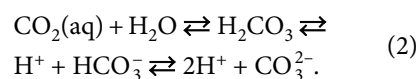
These reactions are very rapid, on time scales of tens of seconds for CO_2 hydration and microseconds for subsequent acid-base reactions (Zeebe and Wolf-Gladrow, 2001; Dickson et al., 2007). In most applications, the partitioning of inorganic carbonate species can be assumed to be in equilibrium. For typical surface ocean conditions, about 90% of the total dissolved inorganic carbon (DIC) occurs as bicarbonate ions (HCO_3^-) and ~ 9% as carbonate ions (CO_3^{2-}), with only ~1% remaining as dissolved $CO_2(aq)$ and H_2CO_3. The third key reaction involves the formation and dissolution of solid calcium carbonate minerals ($CaCO_3(s)$):

$$Ca^{2+} + CO_3^{2-} \rightleftarrows CaCO_3(s). \quad (3)$$
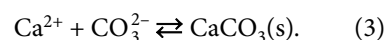
At equilibrium, the calcium concentration times the carbonate concentration is equal to a constant called the apparent solubility product

Richard A. Feely *(richard.a.feely@noaa.gov) is Senior Scientist, Pacific Marine Environmental Laboratory, National Oceanic and Atmospheric Administration, Seattle, WA, USA.* **Scott C. Doney** *is Senior Scientist, Marine Chemistry and Geochemistry, Woods Hole Oceanographic Institution, Woods Hole, MA, USA.* **Sarah R. Cooley** *is Postdoctoral Investigator, Marine Chemistry and Geochemistry, Woods Hole Oceanographic Institution, Woods Hole, MA, USA.*

$([Ca^{2+}] \times [CO_3^{2-}] = K'_{sp})$. The saturation state of calcium carbonate mineral phases is defined by $\Omega = [Ca^{2+}][CO_3^{2-}] / K'_{sp}$. The apparent solubility product varies with temperature, salinity, and pressure, and differs among calcium carbonate minerals (e.g., calcite, aragonite, and high-Mg calcite; Mucci, 1983). The final important reaction is photosynthesis and respiration/decomposition:

$$CO_2 + H_2O \rightleftarrows CH_2O + O_2. \quad (4)$$

As CO_2 concentrations increase in seawater, the CO_2 gas reacts with water to form H_2CO_3. Most of the H_2CO_3 dissociates to form a H^+ and a HCO_3^-, and most of the resulting H^+ reacts with CO_3^{2-} to produce additional HCO_3^- ions. As a result, CO_2 dissolution in the ocean increases H^+ (and thus decreases pH) and decreases CO_3^{2-} concentrations.

The decrease in CO_3^{2-} reduces the saturation state of $CaCO_3$, which directly affects the ability of some $CaCO_3$-secreting organisms, such as planktonic coccolithophores and pteropods, and invertebrates such as mollusks and corals, to produce their shells or skeletons (Equation 3, and Doney et al., 2009). This is true even though most surface waters in the global ocean are currently supersaturated with respect to $CaCO_3$ (e.g., oceanic Ω values of 2–4 for aragonite and 4–6 for calcite, where $\Omega = 1$ expresses saturation), because of the exceedingly slow abiotic precipitation rates for $CaCO_3$ minerals (Table 1). When seawater is supersaturated with respect to aragonite and calcite (saturation levels > 1), calcification is favored more than dissolution. Many organisms have optimal calcium carbonate precipitation rates at the supersaturated states for these minerals that

are characteristic of the pre-industrial ocean, and therefore decreasing CO_3^{2-} concentrations could decrease calcification rates for a number of these species.

Over longer time scales, the ocean's capacity for absorbing more CO_2 from the atmosphere also depends on the extent of marine carbonate interactions with CO_2 via the dissolution reaction:

$$CO_2 + CaCO_3 + H_2O$$
$$\rightleftarrows 2HCO_3^- + Ca^{2+}. \quad (5)$$
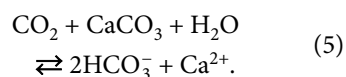
The increase in total alkalinity (TA) from this reaction enhances the ocean's capacity to absorb more CO_2 from the atmosphere (Zeebe and Wolf-Gladrow, 2001). TA is a measure of the excess cations (such as Ca^{2+} and Mg^{2+}) that are balanced by the anions formed by dissociations of carbonic, boric, and other weak acids in seawater. The primary contributors to the dissolution reaction in Equation 5 are the carbonate shells that are produced in the euphotic zone. Upon a calcifying organism's death, its carbonate shell falls through the water column and is either deposited in sediments or dissolved.

The saturation states of carbonate minerals naturally decrease with depth as total dissolved CO_2 increases because of biological respiration and cold temperatures in deep seawater. Below about 1500 m, the depth of the saturation

horizon is governed primarily by the pressure effect on $CaCO_3$ solubility. The shells and skeletons of the unprotected $CaCO_3$ phases begin to dissolve when the degrees of saturation of their component minerals drop below $\Omega = 1$, so some of these shells and skeletons dissolve before reaching deep sediments below the "saturation horizon," or the depth where seawater becomes undersaturated with respect to $CaCO_3$. The locations of the saturation horizons where $\Omega = 1$ differ for different carbonate minerals, varying the response of materials composed of aragonite, calcite, or high-magnesium carbonate. As the ocean becomes enriched in anthropogenic CO_2, the locations in the ocean where dissolution occurs will increase as a function of the decrease in $CaCO_3$ saturation state.

The $\Omega = 1$ chemical threshold is a useful indicator but not a strict criterion for biomineralization and dissolution. Some calcifying organisms require ambient seawater conditions well above saturation, while others may be

> **THE UPTAKE OF ANTHROPOGENIC CO_2 BY THE GLOBAL OCEAN INDUCES FUNDAMENTAL CHANGES IN SEAWATER CHEMISTRY THAT COULD HAVE DRAMATIC IMPACTS ON BIOLOGICAL ECOSYSTEMS IN THE UPPER OCEAN.**

able to generate or maintain calcified structures in undersaturated conditions at a bioenergetic cost. Similarly, $CaCO_3$ dissolution can occur in the water column above the saturation horizon in more acidic microenvironments such as marine snow particles and zooplankton guts.

DATA SETS AND MODELING APPROACH

From 1990 through 1998, carbon system measurements were made on 99 WOCE/JGOFS (World Ocean Circulation Experiment/Joint Global Ocean Flux Study) CO_2 survey cruises in the global ocean (Key et al., 2004; Sabine et al., 2005). These cruises were conducted as a collaborative effort among 15 laboratories from eight countries. At least two carbon parameters were measured on all the cruises, but the carbon system pairs that were measured varied between cruises. The overall accuracy of the DIC data was ±3 µmol kg^{-1}, and for TA, the second most common carbon parameter analyzed, the overall accuracy was ±5 µmol kg^{-1}.

The data were corrected for systematic biases between cruises and maintained as a unique corrected data set (hereafter called GLODAP), which consists of about 72,000 sample locations where DIC and TA were collected. The data are available from the Carbon Dioxide Information Analysis Center (http://cdiac.esd.ornl.gov/oceans/).

The National Center for Atmospheric Research (NCAR) Community Climate System Model 3.1 (CCSM3) was used to estimate the long-term changes in the saturation state of seawater with

Table 1. Average concentrations of carbon system parameters and temperature-and-salinity values for surface waters of the major ocean basins based on the Global Ocean Data Analysis Project data set.

Ocean	[1]Salinity	[1]Temperature (°C)	[2]Dissolved Inorganic Carbon (µmol kg^{-1})	[2]Alkalinity (µmol kg^{-1})	[3]pH (Seawater Scale)	[3]Carbonate Ion (µmol kg^{-1})	[3]Ω_{ar}	[3]Ω_{ca}
[4]Arctic Ocean North of 65°N	34.639 ± 0.53	4.35 ± 3.0	2069.7 ± 36	2299.7 ± 27	8.231 ± 0.06	160.4 ± 18	2.41 ± 0.3	3.82 ± 0.4
North Atlantic 60°W to 0° 0° to 64.5°N	35.643 ± 1.37	19.56 ± 7.3	2040.1 ± 38	2355.8 ± 48	8.125 ± 0.06	222.7 ± 34	3.47 ± 0.6	5.31 ± 0.8
South Atlantic 70°W to 20°E 0° to 40°S	36.022 ± 0.79	22.54 ± 3.7	2045.4 ± 25	2379.9 ± 36	8.102 ± 0.03	236.6 ± 22	3.70 ± 0.4	5.63 ± 0.5
North Pacific 120°E to 60°W 0° to 59.5°N	34.051 ± 0.86	20.81 ± 8.1	1959.3 ± 42	2255.0 ± 34	8.105 ± 0.06	208.1 ± 38	3.30 ± 0.7	5.04 ± 0.9
South Pacific 120°E to 70°W 0° to 40°S	35.287 ± 0.55	23.29 ± 4.3	2003.0 ± 39	2319.3 ± 35	8.079 ± 0.03	223.4 ± 25	3.52 ± 0.4	5.36 ± 0.6
North Indian 20°E to 120°E 0° to 24.5°N	34.722 ± 1.57	28.12 ± 0.8	1951.6 ± 64	2298.2 ± 68	8.068 ± 0.03	244.4 ± 12	3.94 ± 0.2	5.93 ± 0.3
South Indian 20°E to 120°E 0° to 40°S	35.103 ± 0.47	23.46 ± 4.3	1983.8 ± 54	2306.0 ± 36	8.092 ± 0.03	227.0 ± 19	3.59 ± 0.4	5.46 ± 0.5
Southern Ocean South of 40°S	34.775 ± 0.94	16.74 ± 10.5	2034.5 ± 77	2306.9 ± 45	8.102 ± 0.04	193.1 ± 54	3.02 ± 0.9	4.64 ± 1.3
All	34.680 ± 1.02	16.09 ± 10.4	2033.7 ± 75	2302.7 ± 48	8.108 ± 0.05	190.6 ± 53	2.98 ± 0.9	4.58 ± 1.3

Note: the ± values in the table give the standard deviations about the regional means.

[1] World Ocean Atlas 2005 data for time period: Annual, http://www.nodc.noaa.gov/OC5/WOA05/pr_woa05.html

[2] GLODAP version 1.1 gridded data, http://cdiac.ornl.gov/oceans/glodap/data_files.htm

[3] Calculated values using co2sys.xls, http://www.ecy.wa.gov/programs/eap/models/co2sys_ver14.zip

[4] Arctic Ocean data (N=70) from GLODAP version 1.1 bottle data, http://cdiac.ornl.gov/oceans/glodap/data_files.htm

respect to aragonite and calcite (Doney et al., 2006; Steinacher et al., 2009). The modeled decadal mean values were calculated using modeled monthly dissolved inorganic carbon, alkalinity, temperature, and salinity output from CCSM3, which uses full carbon cycle–climate radiative feedbacks and assumes historical fossil fuel emissions and the IPCC Special Report on Emissions Scenarios (SRES) nonintervention future A2 scenario (Thornton et al., 2009). The model's variable grid (0.9–3.6° latitude x 3.6° longitude) was interpolated to a 2° x 2° regular grid for analysis. GLODAP 1° x 1° gridded surface dissolved inorganic carbon and total alkalinity (http://cdiac.ornl.gov/oceans/glodap/Glodap_home.htm) and World Ocean Atlas 2005 (http://www.nodc.noaa.gov/OC5/WOA05/pr_woa05.html) 1° x 1° gridded temperature and salinity data were used to calculate GLODAP-based carbonate system parameters. For both CCSM3 and GLODAP-based data sets, carbonate system parameters were calculated using a standard polynomial solver by Richard Zeebe (University of Hawaii) for Matlab (http://www.soest.hawaii.edu/oceanography/faculty/zeebe_files/CO2_System_in_Seawater/csys.html) and the thermodynamic carbonate dissociation constants from Mehrbach et al. (1973) (refit by Lueker et al., 2000), total pH scale, and other dissociation constants reviewed in Zeebe and Wolf-Gladrow (2001). Before calculating the difference between GLODAP and CCSM-based carbonate system parameters, GLODAP data were interpolated to the same 2° x 2° regular grid as CCSM3 data.

RESULTS AND DISCUSSION

Calcification or dissolution of both planktonic and benthic calcifying organisms commonly depends on the carbonate ion concentration, often expressed by the degree of saturation of the biominerals aragonite and calcite (see Feely et al., 2004, and references therein). Consequently, spatial and temporal changes in saturation state with respect to these mineral phases are important for understanding how ocean acidification might impact future ecosystems. Figures 2 and 3 show mean ocean surface pH and CO_3^{2-} concentrations for the Pacific, Atlantic, and
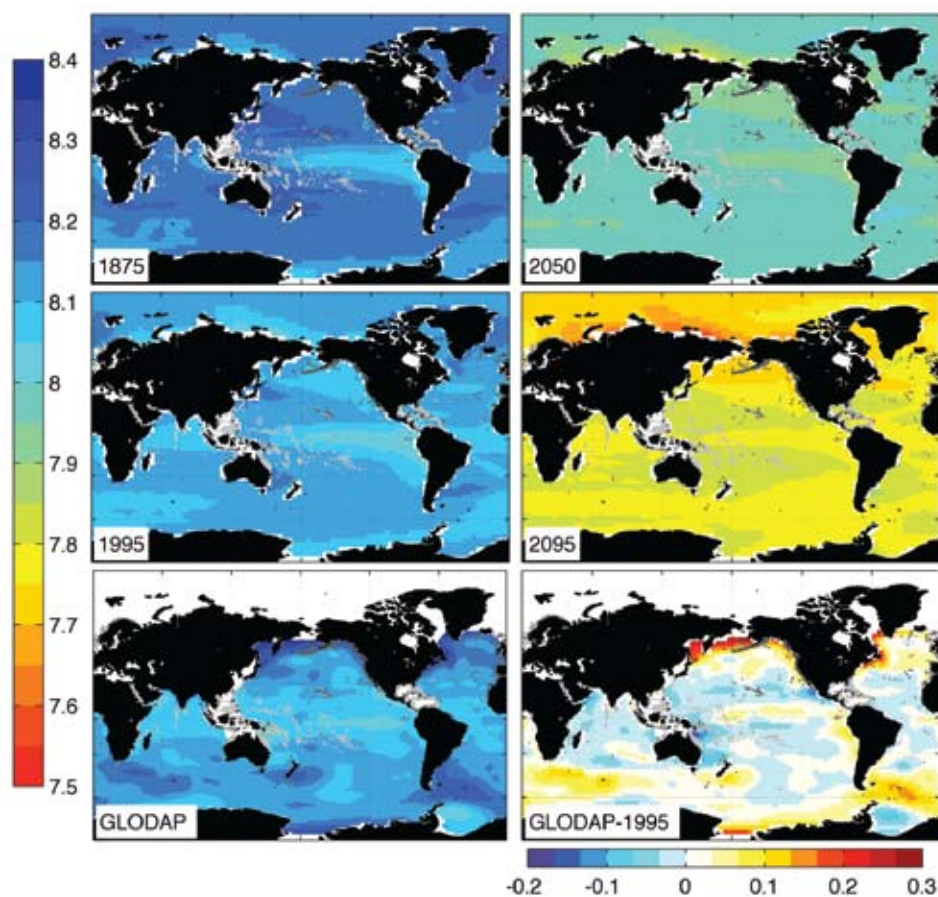

Figure 2. (Top and middle rows) National Center for Atmospheric Research Community Climate System Model 3.1 (CCSM3)-modeled decadal mean pH at the sea surface centered around the years 1875, 1995, 2050, and 2095. (Bottom left) Global Ocean Data Analysis Project (GLODAP)-based pH at the sea surface, nominally for 1995. (Bottom right) The difference between the GLODAP-based and CCSM-based 1995 fields. Note the different range of the difference plot. Deep coral reefs are indicated by darker gray dots; shallow-water coral reefs are indicated with lighter gray dots. White areas indicate regions with no data.
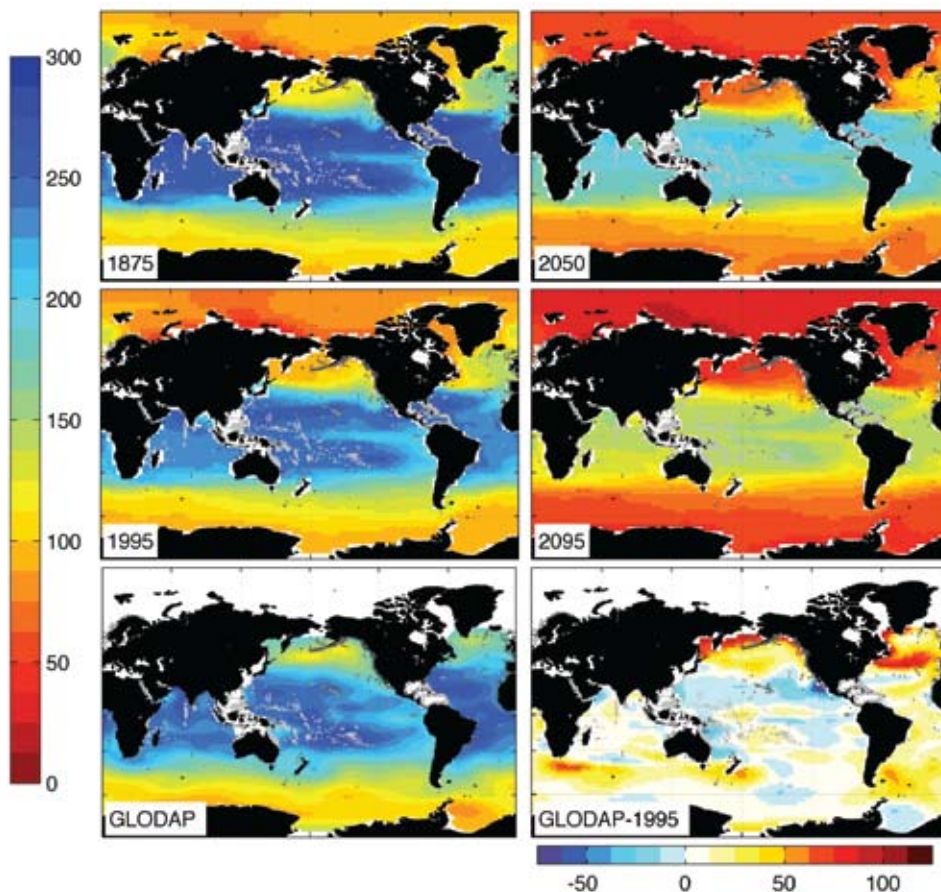
Indian oceans from the CCSM3 model projections for the decades centered on 1875, 1995, 2050, and 2095, as well as the difference between the GLODAP gridded data and the 1995 model results, respectively. Based on the GLODAP data set, open-ocean surface water pH ranges from about 7.95–8.35 (mean = 8.11); CO_3^{2-} concentrations range from about 80–300 µmol kg^{-1} (mean = 191 µmol kg^{-1}); aragonite saturation values range from approximately 2.4–3.9; and calcite saturation from approximately 3.8–5.9 (Table 1). GLODAP pH and carbonate ion values are higher in highly productive regions of the western North and South Atlantic, western North and South Pacific, South Indian Ocean, Bering Sea, and most of the Southern Ocean (Figures 2 and 3). These regions have a large uptake of

CO_2 (high pH, high CO_3^{2-}) during the spring–summer months when productivity is strongest and when most of the surveys occurred. Because the modeled results for 1995 are decadal averages, it is not too surprising that the largest data-model differences occur in these highly productive subpolar regions.

Model projections indicate that surface ocean pH will drop from a pre-industrial average of about 8.2 to a mean of about 7.8 in the IPCC A2 scenario by the end of this century. For CO_3^{2-}, the highest concentrations are in the tropical and subtropical regions, particularly on the western side of each basin where the waters are warmer and saltier. For most open-ocean surface waters, aragonite undersaturation occurs when CO_3^{2-} concentrations drop below approximately 66 µmol kg^{-1}. Model

projections suggest that this will start to occur at about 2020 in the Arctic Ocean (Steinacher et al., 2009) and 2050 in the Southern Ocean south of 65°S (Orr et al., 2005) in the A2 business-as-usual scenario. By 2050, all of the Arctic will be undersaturated with respect to aragonite (Figure 4), and by 2095, all of the Southern Ocean south of 60°S and parts of the North Pacific will be undersaturated. In the Arctic Ocean, the rapid decrease in saturation state occurs, in part, as a direct result of the decrease in TA in surface waters due to the increase in freshwater inflow from low-alkalinity river water and from ice melt (Orr et al., 2005). For calcite, undersaturation occurs when CO_3^{2-} drops below 42 µmol kg^{-1} (Figure 5). By 2095, most of the Arctic and some parts of the Bering and Chukchi seas will be undersaturated
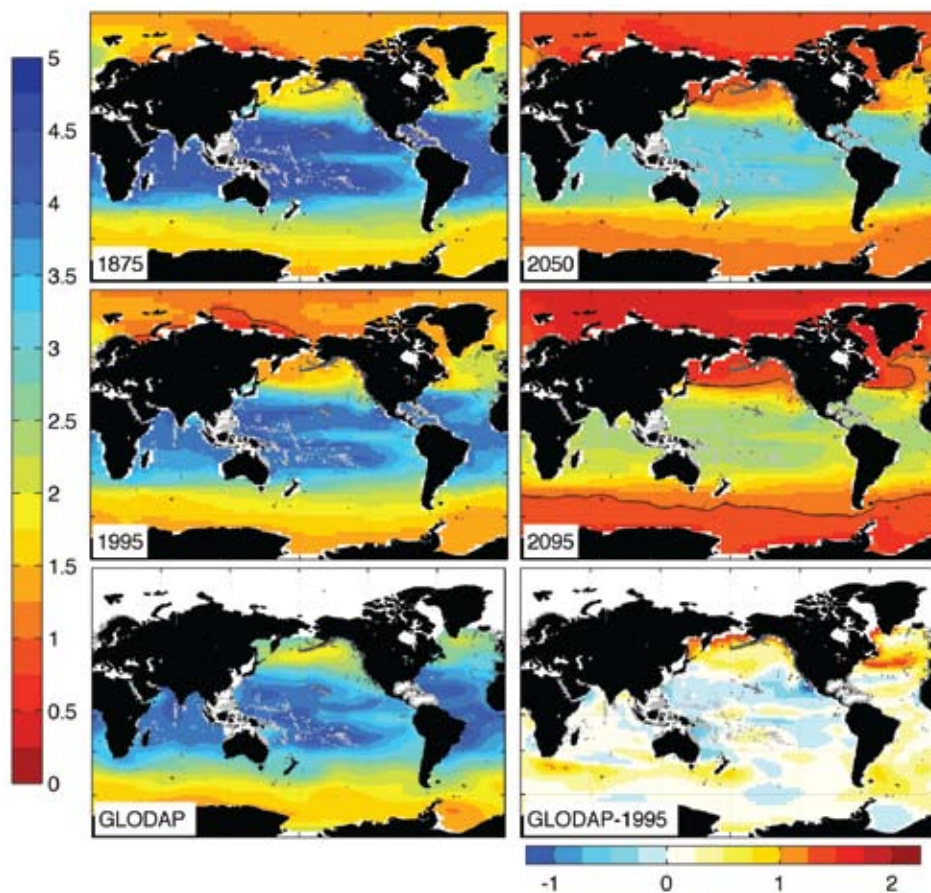
Figure 4. (Top and middle rows) CCSM3-modeled decadal mean Ω_{ar} at the sea surface, centered around the years 1875, 1995, 2050, and 2095. (Bottom left) GLODAP-based Ω_{ar} at the sea surface, nominally for 1995. (Bottom right) The difference between the GLODAP-based and CCSM-based 1995 fields. Note the different range of the difference plot. Deep coral reefs are indicated by darker gray dots; shallow-water coral reefs are indicated with lighter gray dots. White areas indicate regions with no data.

Figure 5. (Top and middle rows) CCSM3-modeled decadal mean Ω_{ca} at the sea surface centered around the years 1875, 1995, 2050, and 2095. (Bottom left) GLODAP-based Ω_{ca} at the sea surface, nominally for 1995. (Bottom right) The difference between the GLODAP-based and CCSM-based 1995 fields. Note the different range of the difference plot. Deep coral reefs are indicated by darker gray dots; shallow-water coral reefs are indicated with lighter gray dots. White areas indicate regions with no data.
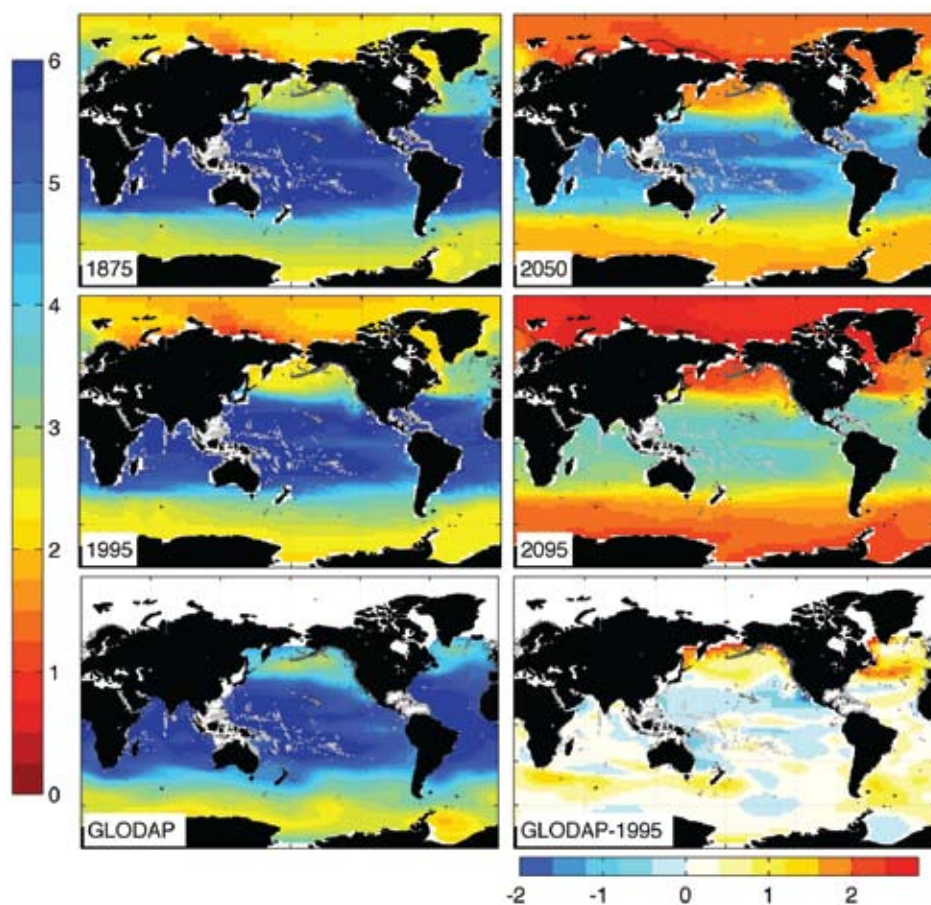
with respect to calcite. However, in most of the other ocean basins the surface waters will still be oversaturated with respect to calcite, but at a level greatly reduced from the present.

In Figure 6, average basin-wide saturation state profiles for aragonite (solid line) and calcite (dashed line) are plotted along with depth profiles of pH and CO_3^{2-} concentrations for each of the basins (Figure 6). The depth profiles show that both pH and CO_3^{2-} decrease rapidly in subsurface waters because of the release of CO_2, primarily from circulation and respiration processes within the subsurface water masses. Portions of the eastern subtropical Atlantic become undersaturated with respect to aragonite between 400 and 1000 m, and all of the Atlantic becomes undersaturated with respect to calcite below a depth of approximately 3000–3500 m (Chung et al., 2004; Feely et al., 2004). In the Indian and Pacific oceans, undersaturation of aragonite begins at much shallower depths where the CO_3^{2-} drops below a value of about 66 μmol kg^{-1} (depth range of 100–1200 m, depending on location) because the waters are much older and have acquired more CO_2 from the cumulative effects of respiration while they travel along the transport pathway of the deeper water masses. The calcite saturation depths in the Indian and Pacific are generally about 50–200 m deeper than the aragonite saturation depth. The addition of anthropogenic CO_2 over the past 250 years has caused the aragonite saturation horizons to shoal toward the surface in all ocean basins by varying amounts, ranging from about 50–200 m, depending on location (Feely et al., 2004; Orr et al., 2005).

Because aragonite and calcite saturation values are highest in warm tropical and subtropical oceans, these regions might also experience the largest absolute changes in saturation state by the end of the century. Figure 7 and Table 2 show the projected absolute and relative changes, or fractional changes, of aragonite state from 1865 to 2095. The largest projected decreases in aragonite saturation between 1865 and 2095 are observed in warm tropical and subtropical waters (Figure 7, top). For example,
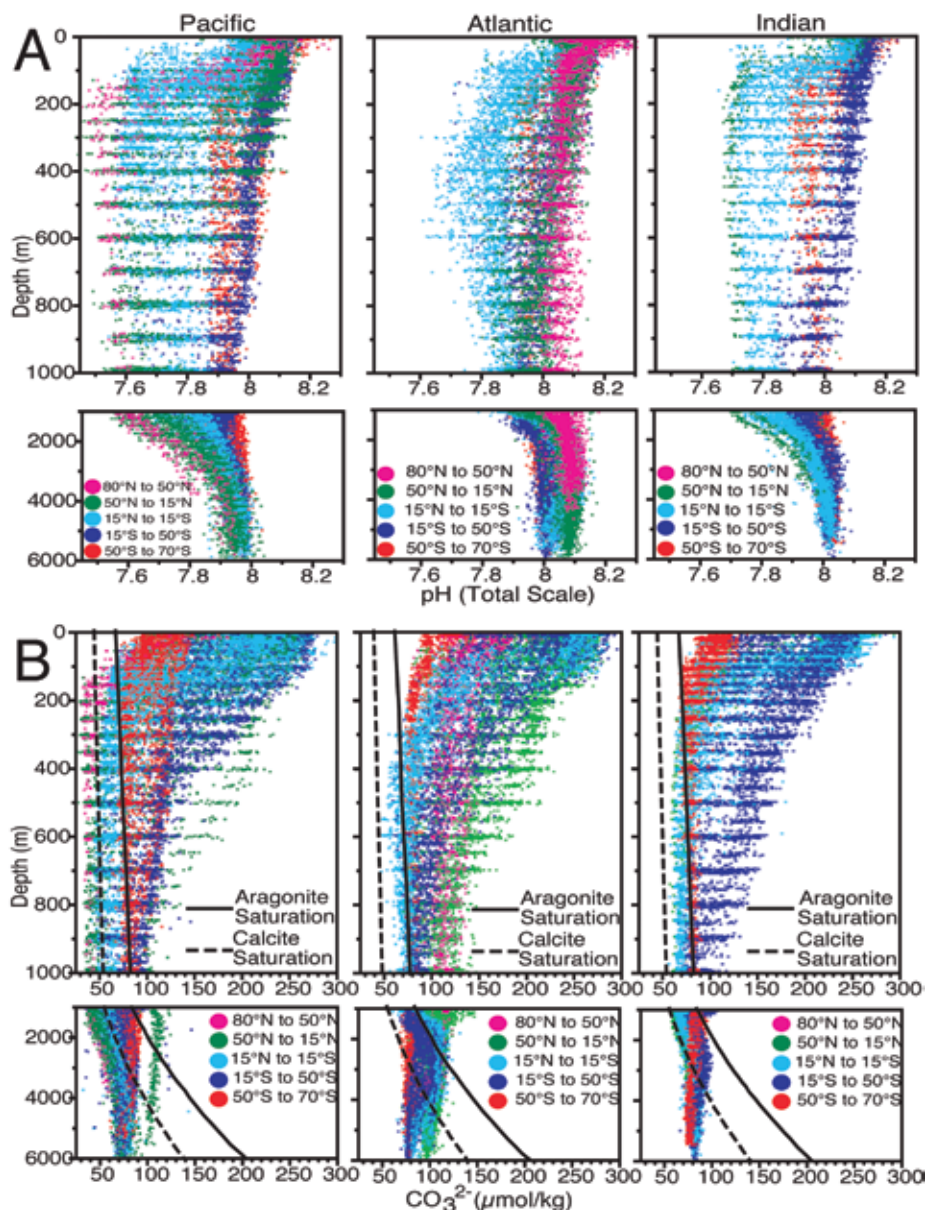

Figure 6. Distribution of: (A) pH and (B) CO_3^{2-} concentration in the Pacific, Atlantic, and Indian oceans. The data are from the World Ocean Circulation Experiment/Joint Global Ocean Flux Study/Ocean Atmosphere Carbon Exchange Study global CO_2 survey data (Sabine et al., 2005). The lines show the average aragonite (solid line) and calcite (dashed line) saturation CO_3^{2-} concentration for each of these basins. The color coding shows the latitude bands for the data sets (after Feely et al., 2009).
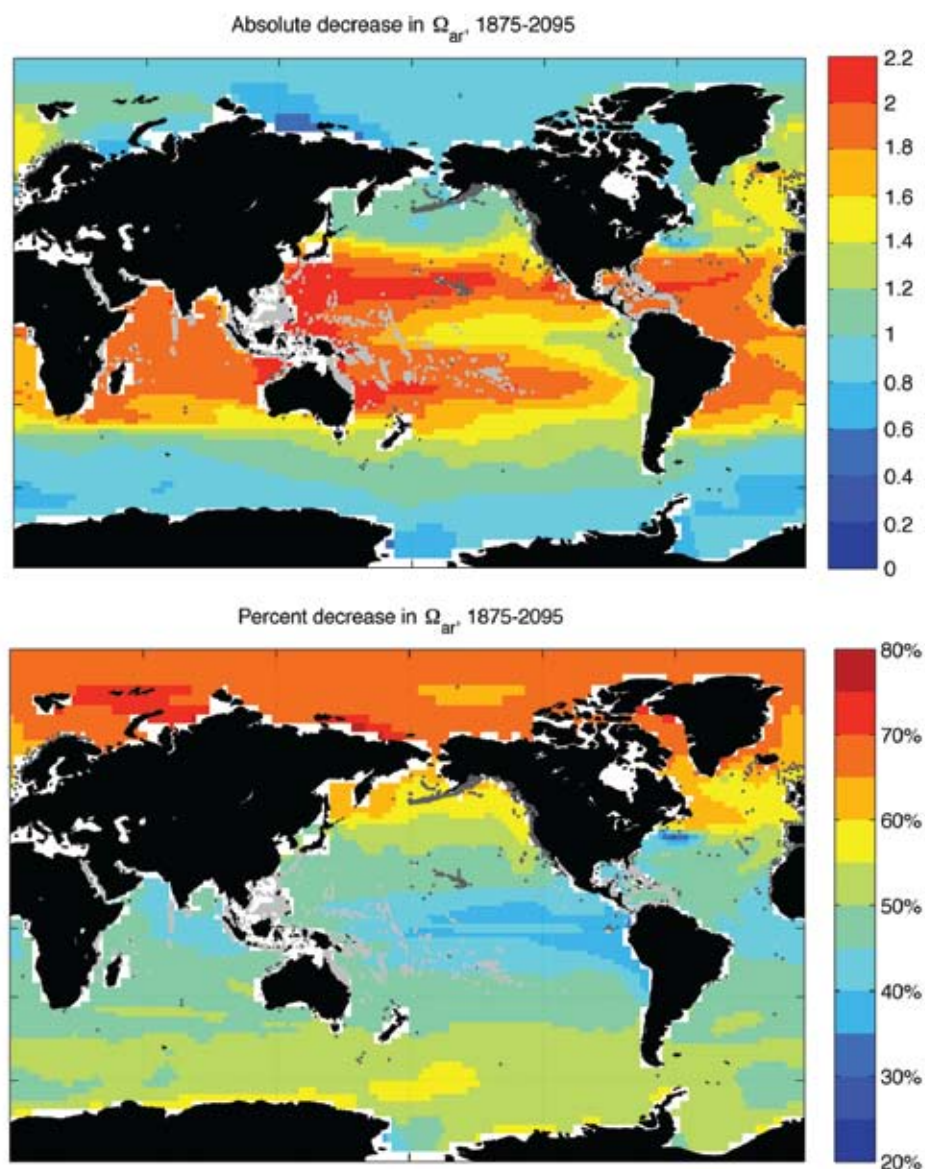
Figure 7. For the Intergovernmental Panel on Climate Change Special Report on Emissions Scenarios A2 scenario, (top) the CCSM-modeled decrease in surface Ω_{ar} between the decades centered around the years 1875 and 2095 ($\Delta\Omega_{ar} = \Omega_{ar, 1875} - \Omega_{ar, 2095}$), and (bottom) the CCSM-modeled percent decrease in surface Ω_{ar} between the decades centered around 1875 and 2095 ($100 \times \Delta\Omega_{ar, 2095} / \Omega_{ar, 1875}$). Deep coral reefs are indicated by darker gray dots; shallow-water coral reefs are indicated with lighter gray dots. White areas indicate regions with no data.

et al., 2009), implying that future low-latitude conditions could stress tropical species by significantly altering the conditions to which they have adapted.

On the other hand, the relative changes in CO_3^{2-} concentrations and aragonite and calcite saturation states are highest in the high latitudes. There, the large changes in carbonate chemistry relative to historical conditions, which are captured in both the large percent changes in modeled carbonate system parameters and the saturation state changes from supersaturation ($\Omega > 1$) to undersaturation ($\Omega < 1$), might have large impacts on high-latitude calcifying planktonic and benthic organisms such as pteropods, mussels, and oysters (Fabry et al., 2008; Doney et al., 2009). Whether absolute or relative changes in CO_3^{2-} concentrations and/or aragonite and calcite saturation state play a controlling role in overall ecosystem changes has yet to be determined. Nevertheless, the striking decreases in aragonite and calcite saturation state projected by the end of this century over the entire ocean clearly indicate that there is a reasonable cause for concern.

CONCLUSIONS

The oceanic uptake of anthropogenic CO_2 from the atmosphere is decreasing the pH and lowering the CO_3^{2-} concentration and $CaCO_3$ saturation states of aragonite and calcite in the upper ocean. Ocean acidification is expected to result in a pH decrease of ~ 0.3–0.4 units relative to pre-industrial values by the end of this century. Based on the best available information and model projections, it appears that as levels of dissolved CO_2 in seawater rise, the skeletal growth rates of calcium-secreting organisms will be

in the tropical and subtropical Atlantic, the average decrease in aragonite saturation state between the present-day levels and a 3XCO_2-world (~ 840 µatm) is -0.81, whereas in the high-latitude North Atlantic, it is only -0.39 (Table 2). The temperate latitude differences are generally somewhere in the middle between

these two extremes. In the tropics and subtropics, many species of tropical corals are extremely sensitive to any decreases in saturation state (Langdon, 2002). In these same locations, natural variability in the ocean carbonate system is much smaller than forecasted anthropogenically driven changes (Cooley

Table 2. Absolute and relative changes in pH, carbonate ion, and aragonite and calcite saturation states for 2X and 3X pre-industrial CO_2 levels at various locations in the Atlantic and Pacific oceans based on National Center for Atmospheric Research Community Climate System Model 3.1 results.

Location	fCO₂ µatm	pH	Δ pH	Carbonate ion µmol kg⁻¹	Δ Carbonate	% Change	Ω_ar	Δ Ω_ar	% Change	Ω_ca	Δ Ω_ca	% Change
North Atlantic > 50°N	387	8.040		96.8			1.47			2.34		
	560	7.893	-0.15	71.2	-25.6	-26.5	1.08	-0.39	-26.5	1.72	-0.62	-26.5
	840	7.727	-0.31	49.9	-46.9	-48.4	0.76	-0.71	-48.4	1.21	-1.13	-48.4
North Pacific > 50°N	387	8.032		92.3			1.40			2.24		
	560	7.885	-0.15	67.8	-24.5	-26.5	1.03	-0.37	-26.5	1.65	-0.59	-26.5
	840	7.719	-0.31	47.5	-44.8	-48.5	0.72	-0.68	-48.5	1.15	-1.09	-48.5
Tropical Atlantic	387	8.055		237.5			3.85			5.81		
	560	7.923	-0.13	187.5	-50.0	-21.0	3.04	-0.81	-21.0	4.59	-1.22	-21.0
	840	7.772	-0.28	140.6	-97.0	-40.8	2.28	-1.57	-40.8	3.44	-2.37	-40.8
Tropical Pacific	387	8.035		234.4			3.81			5.71		
	560	7.905	-0.13	185.9	-48.5	-20.7	3.02	-0.79	-20.7	4.53	-1.18	-20.7
	840	7.755	-0.28	139.9	-94.5	-40.3	2.28	-1.54	-40.3	3.41	-2.30	-40.3
Subpolar Atlantic	387	8.052		169.3			2.59			4.02		
	560	7.913	-0.14	129.4	-39.9	-23.6	1.98	-0.61	-23.6	3.07	-0.95	-23.6
	840	7.756	-0.30	93.9	-75.3	-44.5	1.44	-1.15	-44.5	2.23	-1.79	-44.5
Subpolar Pacific	387	8.038		134.5			2.06			3.24		
	560	7.896	-0.14	101.3	-33.2	-24.7	1.55	-0.51	-24.7	2.44	-0.80	-24.7
	840	7.736	-0.30	72.5	-62.0	-46.1	1.11	-0.95	-46.1	1.75	-1.49	-46.1

reduced due to the effects of decreased ocean CO_3^{2-} concentrations. If anthropogenic CO_2 emissions are not dramatically reduced in the coming decades, there is the potential for direct and profound impacts on our living marine ecosystems.

REFERENCES

Bates, N.R. 2007. Interannual variability of the oceanic CO_2 sink in the subtropical gyre of the North Atlantic Ocean over the last 2 decades. *Journal of Geophysical Research* 112, C09013, doi:10.1029/2006JC003759.

Bates, N.R., and A.J. Peters. 2007. The contribution of atmospheric acid deposition to ocean acidification in the subtropical North Atlantic Ocean. *Marine Chemistry* 107(4):547–558.

Broecker, W., and E. Clarke. 2001. A dramatic Atlantic dissolution event at the onset of the last glaciation. *Geochemistry Geophysics Geosystems* 2(11):1,065, doi:10.1029/2001GC000185.

Caldeira, K., and M.E. Wickett. 2003. Anthropogenic carbon and ocean pH. *Nature* 425(6956):365.

Caldeira, K., and M.E. Wickett. 2005. Ocean model predictions of chemistry changes from carbon dioxide emissions to the atmosphere and ocean. *Journal of Geophysical Research* 110, C09S04, doi:10.1029/2004JC002671.

Canadell, J.G., C. Le Quéré, M.R. Raupach, C.B. Field, E.T. Buitenhuis, P. Ciais, T.J. Conway, N.P. Gillett, R.A. Houghton, and G. Marland. 2007. Contributions to accelerating atmospheric CO_2 growth from economic activity, carbon intensity, and efficiency of natural sinks. *Proceedings of the National Academy of Sciences of the United States of America* 104(47):18,866–18,870, doi:10.1073pnas.0702737104.

Chung, S.N., G.-H. Park, K. Lee, R.M. Key, F.J. Millero, R.A. Feely, C.L. Sabine, and P.G. Falkowski. 2004. Postindustrial enhancement of aragonite undersaturation in the upper tropical and subtropical Atlantic Ocean: The role of fossil fuel CO_2. *Limnology and Oceanography* 49(2):315–321.

Cooley, S.R., H.L. Kite-Powell, and S.C. Doney. 2009. Ocean acidification's potential to alter global marine ecosystem services. *Oceanography* 22(4):172–181.

Dickson, A.G., C.L. Sabine, and J.R. Christian, eds. 2007. Guide to Best Practices for Ocean CO_2 Measurements. PICES Special Publication 3, 191 pp.

Doney, S.C., V.J. Fabry, R.A. Feely, and J.A. Kleypas. 2009. Ocean acidification: The other CO_2 problem. *Annual Reviews of Marine Science* 1:169–192.

Doney, S.C., K. Lindsay, I. Fung, and J. John. 2006. Natural variability in a stable 1000 year coupled climate-carbon cycle simulation. *Journal of Climate* 19(13):3,033–3,054.

Dore, J.E., R. Lukas, D.W. Sadler, M.J. Church, and D.M. Karl. 2009. Physical and biogeochemical modulation of ocean acidification in the central North Pacific. *Proceedings of the National Academy of Sciences of the United States of America* 106(30):12,235–12,240.

Fabry, V.J., B.A. Seibel, R.A. Feely, and J.C. Orr. 2008. Impacts of ocean acidification on marine fauna and ecosystem processes. *ICES Journal of Marine Science* 65(3):414–432.

Feely, R.A., J. Orr, V.J. Fabry, J.A. Kleypas, C.L. Sabine, and C. Langdon. 2009. Present and future changes in seawater chemistry due to ocean acidification. Section 3 in *Carbon Sequestration and Its Role in the Global Carbon Cycle*. B.J. McPherson and E.T. Sundquist, eds, Geophysical Monograph Series, Vol. 83, American Geophysical Union, Washington, DC.

Feely, R.A., C.L. Sabine, K. Lee, W. Berelson, J. Kleypas, V.J. Fabry, and F.J. Millero. 2004. Impact of anthropogenic CO_2 on the $CaCO_3$ system in the oceans. *Science* 305(5682):362–366, doi:10.1126/science.1097329.

Friedlingstein, P., P. Cox, R. Betts, C. Jones, W. von Bloh, V. Brovkin, P. Cadule, S. Doney, M. Eby, D. Matthews, and others. 2006. Climate-carbon cycle feedback analysis: Results from the C*MIP model intercomparison. *Journal of Climate* 19(14):3,337–3,353.

Key, R.M., A. Kozyr, C.L. Sabine, K. Lee, R. Wanninkhof, J.L. Bullister, R.A. Feely, F.J. Millero, C. Mordy, and T.-H. Peng. 2004. A global ocean carbon climatology: Results from Global Data Analysis Project (GLODAP). *Global Biogeochemical Cycles* 18, GB4031, doi:10.1029/2004GB002247.

Langdon, C. 2002. Review of experimental evidence for effects of CO_2 on calcification of reef builders. *Proceedings of the 9th International Coral Reef Symposium* 2:1,091–1,098 (Symposium met October 23–27, 2000, in Bali, Indonesia).

Lueker, T.J., A.G. Dickson, and C.D. Keeling. 2000. Ocean pCO_2 calculated from dissolved inorganic carbon, alkalinity, and equations for K-1 and K-2: Validation based on laboratory measurements of CO_2 in gas and seawater at equilibrium. *Marine Chemistry* 70(1–3):105–119.

Lüthi, D., M. Le Floch, B. Bereiter, T. Blunier, J.-M. Barnola, U. Siegenthaler, D. Raynaud, J. Jouzel, H. Fischer, K. Kawamura, and T.F. Stocker. 2008. High-resolution carbon dioxide concentration record 650,000–800,000 years before present. *Nature* 453:379–382.

Mehrbach, C., C.H. Culberson, J.E. Hawley, and R.M. Pytkowicz, 1973. Measurement of the apparent dissociation constants of carbonic acid at atmospheric pressure. *Limnology and Oceanography* 18:897–907.

Mucci, A. 1983. The solubility of calcite and aragonite in seawater at various salinities, temperatures, and one atmosphere total pressure. *American Journal of Science* 283(7):780–799.

Orr, J.C., V.J. Fabry, O. Aumont, L. Bopp, S.C. Doney, R.A. Feely, A. Gnanadesikan, N. Gruber, A. Ishida, F. Joos, and others. 2005. Anthropogenic ocean acidification over the twenty-first century and its impact on calcifying organisms. *Nature* 437(7059):681–686.

Sabine, C.L., and R.A. Feely. 2007. The oceanic sink for carbon dioxide. Pp. 31–49 in *Greenhouse Gas Sinks*. D. Reay, N. Hewitt, J. Grace, and K. Smith, eds, CABI Publishing, Oxfordshire, UK.

Sabine, C.L., R.M. Key, A. Kozyr, R.A. Feely, R. Wanninkhof, F.J. Millero, T.-H. Peny, J.L. Bullister, and K. Lee. 2005. *Global Ocean Data Analysis Project (GLODAP): Results and Data*. ORNL/CDIAC-15, NDP-083, Carbon Dioxide Information Analysis Center, Oak Ridge National Laboratory, US Department of Energy, Oak Ridge, TN. Available online at: http://cdiac.ornl.gov/oceans/glodap/pubs.htm (accessed November 13, 2009).

Santana-Casiano, J.M., M. Gonzalez-Davila, M.J. Rueda, O. Llinas, and E.F. Gonzalez-Davila. 2007. The interannual variability of oceanic CO_2 parameters in the Northeast Atlantic subtropical gyre at the ESTOC site. *Global Biogeochemical Cycles* 21, GB1015, doi:10.1029/2006GB002706.

Steinacher, M., F. Joos, T.L. Frolicher, G.-K. Plattner, and S.C. Doney. 2009. Imminent ocean acidification in the Arctic projected with the NCAR global coupled carbon cycle-climate model. *Biogeosciences* 6:515–533.

Takahashi, T., S.C. Sutherland, R. Wanninkhof, C. Sweeney, R.A. Feely, D.W. Chipman, B. Hales, G. Friederich, F. Chavez, C. Sabine, and others. 2009. Climatological mean and decadal change in surface ocean pCO_2, and net sea-air CO_2 flux over the global oceans. *Deep Sea Research Part II* 56(8–10):554–577.

Thornton, P.E., S.C. Doney, K. Lindsay, J.K. Moore, N. Mahowald, J.T. Randerson, I. Fung, J.-F. Lamarque, J.J. Feddema, and Y.-H. Lee. 2009. Carbon-nitrogen interactions regulate climate-carbon cycle feedbacks: Results from an atmosphere-ocean general circulation model. *Biogeosciences* 6:2,099–2,120.

Zeebe, R.E., and D. Wolf-Gladrow. 2001. *CO₂ in Seawater: Equilibrium, Kinetics, Isotopes*. Elsevier Oceanography Series, 65. Elsevier Science, B.V., Amsterdam, 346 pp.